Journal of the Optical Society of America B
OPTICAL PHYSICS

Transit Ramsey EIT resonances in a Rb vacuum cell

Ravn M. Jenkins, Eugeniy E. Mikhailov, and Irina Novikova*

College of William & Mary, Williamsburg, Virginia 23185, USA
*Corresponding author: ixnovi@wm.edu

Received 4 December 2018; revised 25 January 2019; accepted 1 February 2019; posted 4 February 2019 (Doc. ID 354411); published 11 March 2019

We report the observation of a transient spectral feature in a dual-channel arrangement for electromagnetically induced transparency in a vacuum Rb vapor cell, which is caused by consecutive interactions of atoms with the two laser beams while their ground-state spin coherence are preserved. Despite a relatively small fraction of atoms that are participating in this process, their contribution to the overall line shape is not negligible and can be controlled by adjusting the relative phases between the optical fields in the two interaction regions. We also demonstrate that, thanks to the extended spin coherence evolution time, such differential intensity measurements can produce an error signal for the microwave frequency stabilization that is as strong as single-channel measurements. Additionally, the effective cancellation of the intensity noise, which dominates the single-channel detection, results in more than an order of magnitude higher signal-to-noise ratio.

https://doi.org/10.1364/JOSAB.36.000890

1. INTRODUCTION

Two-photon Raman resonances in Rb atoms provide an all-optical access to long-lived spin coherences and enable the realization of the strong coupling regime between light and ensembles of room-temperature atoms [1,2]. Such interactions lead to strong enhancement of non-linear properties necessary for realization of atom-based quantum information components, such as quantum memories [3,4], quantum network nodes [5,6], and sources of squeezed and entangled light [7,8]. At the same time, the resulting spectrally narrow optical transmission and absorption resonances are widely used in precision metrology, for example, in atomic clocks [9–11] and magnetometers [12–14]. All these applications benefit from the longer atomic spin coherence time, which for the thermal atomic ensembles is often limited by the interaction time of moving atoms with the laser beam, since unavoidable collisions with the walls of a vapor cell completely dephase any light-induced spin coherence [15]. There are several strategies to reduce the spin decoherence rate, such as coating inner cell walls with a special anti-relaxation coating [16,17] or introducing an inert buffer gas to increase the interaction time as atoms slowly diffuse through the laser beam [18]. However, each method brings their complications, for example, collisions with the buffer gas also broaden and shift optical transitions, increasing the environmental sensitivity. Plus, some two-photon resonances are degraded by the strong collisional depolarization of the optical excited state, thus deeming the use of a buffer gas impractical.

Here we demonstrate an experimental arrangement, which we call a transit Ramsey electromagnetically induced transparency (TREIT) effect, where we take advantage of the ballistic motion of Rb atoms between two identical illuminated regions to extend the useful evolution time of the spin coherence and thus to obtain an additional narrow spectral feature within a usual two-photon transmission resonance. Each interaction region consists of two optical fields near the two-photon resonant conditions, shown in Fig. 1(a), responsible for electromagnetically induced transparency (EIT) [19], or, as it is often alternatively referred to, coherent population trapping (CPT) [10,11,20]. While the majority of atoms interact only once with each laser beam before hitting the cell wall, a group of atoms can traverse both beams with their spin coherence intact, as depicted in Fig. 1(b). These atoms experience the conditions similar to the original Ramsey experiment [21], as they undergo two consecutive interactions with the laser fields, separated by a free evolution region. This arrangement is also a spatial equivalent of Raman–Ramsey CPT experiments [22–24], as the spin superposition state, prepared in the first beam, is allowed to evolve in the dark before interacting with the second beam. As a result, we observe an additional interference-like feature on top of the regular single-channel EIT resonance, shown in Figs. 1(c) and 1(d). The spectral narrowing associated with such multi-zone interactions has been investigated in the case of degenerate Hanle magneto-optical resonances [25–27].

The TREIT effect, based on the hyperfine spin coherence, allows realization of a differential detection scheme that

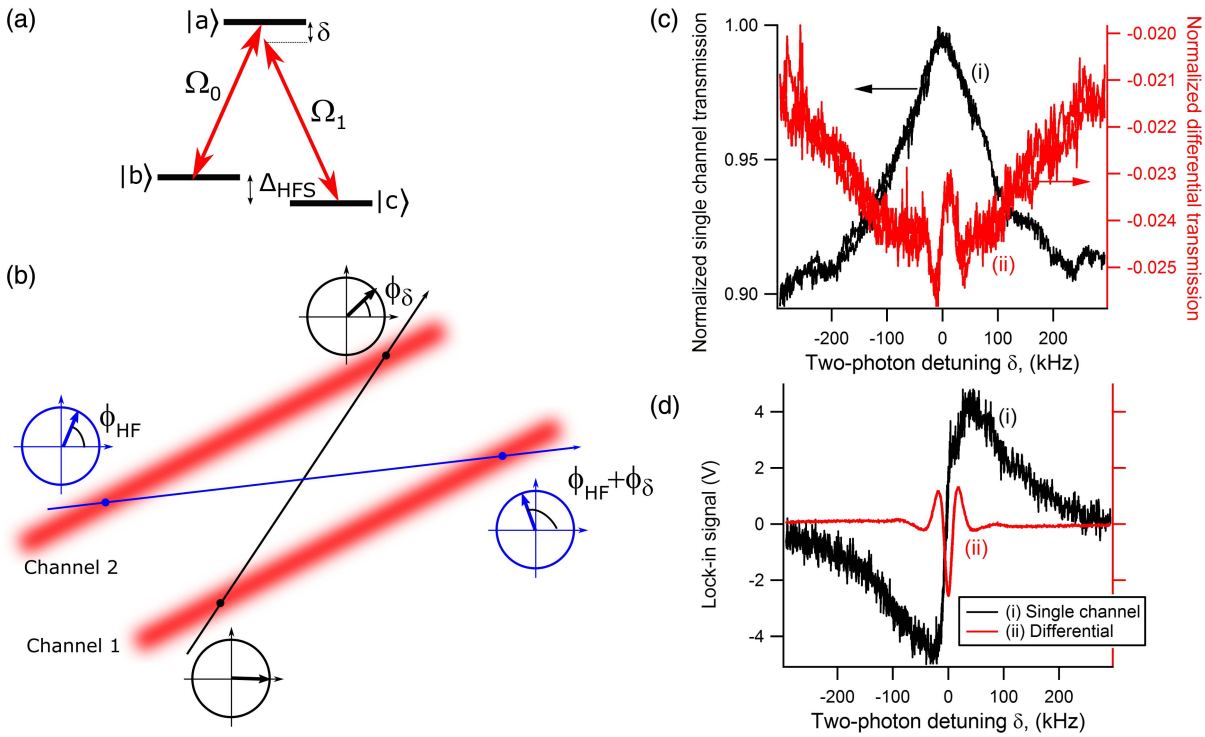

Fig. 1. (a) Schematic EIT level diagram. (b) Simplified geometry of the two-channel transient EIT setup. The arrows in the circles indicate the dark state phases of two atoms traveling symmetrically between the beams. For this illustration we set the phase between the two EIT optical fields to be zero in the first beam and $\phi_{\mathrm{HF}} \neq 0$ for the second beam. In case of the non-zero two-photon detuning $\delta = \omega_1 - \omega_0 - \Delta_{\mathrm{HFS}}$, the dark state phases of both atoms evolve by $\phi_\delta = \delta \cdot \tau$ after τ transit time between the two beams, resulting in the difference in the optical response during the repeated interrogation. (c) Examples of the optical transmission for a single-channel EIT (i) and for the intensity difference between the two channels (ii). Both signals are normalized to the peak EIT transmission in one channel. Small non-zero background in the differential signal is due to imperfect match of the laser beam diameters in the two channels. (d) Same signals recorded using the phase-sensitive lock-in detection.

strongly suppresses the intensity noise, common for both beams. Since the adjustments of the relative phases between the two optical fields allow us to independently control the phases of the spin coherence in each interaction region, it is possible to maximize the difference between the TREIT features in two channels, so that only they are contributing in the differential intensity signal. We found that even though only a small fraction of atoms interacts with both laser beams, their extended coherence evolution and, consequently, the narrower spectral width makes TREIT contribution comparable with the single-channel resonance, especially in the case of the phase-sensitive lock-in detection. At the same time, the cancellation of the intensity noise in this detection scheme results in significantly improved signal-to-noise ratio (SNR).

The potential applications for the TREIT effect, however, are not limited by the improved metrology. For example, it can be used to increase the useful lifetime of atomic spin coherence in the situations when using a buffer gas or anti-relaxation coating is impractical, e.g., in ultra-thin vapor cells [28,29]. The two-zone detection can also be used to unintrusively probe the coherence properties of atoms outside of the main interaction region, or to carefully characterize the extent of the spin coherence migration in any dual-rail or multiplexed experimental arrangements, commonly used in quantum optics [3,30–32].

2. EXPERIMENTAL ARRANGEMENTS

The schematic of the experimental setup is shown in Fig. 2. To create the two optical fields for the EIT resonance, we used a vertical cavity surface-emitting diode laser (VCSEL) operating at the Rb D_1 line (794.7 nm), current-modulated at the frequency of the ^{87}Rb ground-state hyperfine splitting $\nu_{\mathrm{rf}} = \Delta_{\mathrm{HFS}} + \delta$, where $\Delta_{\mathrm{HFS}} \simeq 6.834$ GHz. We locked the carrier frequency of the laser to the $5S_{1/2}F = 2 \rightarrow 5P_{1/2}F' = 1$

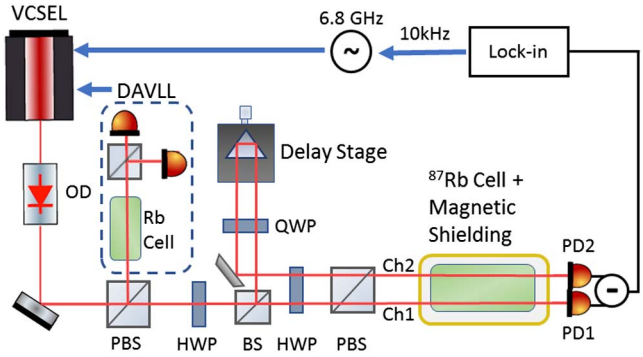

Fig. 2. Schematic of the experimental setup for the differential detection. For a single-channel measurement one of the beams is blocked before the cell. See text for abbreviations.

optical transition with dichroic atomic vapor laser lock (DAVLL), so that the +1 modulation sideband, containing ≈20% of the total laser power became resonant with the $5S_{1/2}F = 1 \rightarrow 5P_{1/2}F' = 1$ transition, forming a Λ system, shown in Fig. 1(a). A detailed description of the VCSEL current modulation and DAVLL arrangements can be found in [33].

After passing through the optical diode, the VCSEL output with a maximum total power of 300 μW was split into two beams using a non-polarizing beam splitter. While the transmitted beam (Ch1) passed directly forward, the reflected beam (Ch2) was directed toward a delay line, consisting of a retro-reflecting prism mounted on a translation stage, before being reflected by a mirror to travel parallel to the first beam at a separation of ≈5 mm. Moving the prism allowed us to adjust the relative phase between the zeroth and the first modulation sidebands inside the Rb cell in the second channel:

$$\phi_{\mathrm{HF}} = 2\pi\Delta z/\lambda_{\mathrm{RF}}, \tag{1}$$

where Δz is the additional path length in the delay stage, and $\lambda_{\mathrm{RF}} = c/\Delta_{\mathrm{HFS}}$ is the wavelength of the resonant frequency between the two hyperfine states. For this experiment we used the lin||lin EIT configuration [33,34]. A polarizing beam splitter placed before the Rb cell ensured the identical linear polarization of all optical fields in both channels. A half-wave plate and a quarter-wave plate before and after the non-polarizing beam splitter allowed us to precisely balance the laser power in two channels. At the cell location, both laser beams had almost identical slightly elliptical Gaussian profiles: the measured $1/e^2$ radii in the first channel were 0.72 mm and 0.75 mm, and in the second channel they were 0.74 mm and 0.72 mm.

Both beams then passed through an evacuated cylindrical Pyrex cell (length 75 mm, diameter 22 mm) containing isotopically enriched ^{87}Rb vapor, heated to 44.5°C. The cell is mounted inside a three-layer magnetic shielding to suppress stray magnetic fields to the level below a few wG and to ensure negligible Zeeman splitting of the magnetic levels. Then, the transmitted light intensities in both channels were detected using two identical photodiodes, PD1 and PD2, that can be operated in the differential mode. We have also recorded the output of the lock-in amplifier by superimposing an additional 10 kHz frequency modulation on the 6.834 GHz VCSEL RF modulation signal.

3. TRANSIENT RAMSEY RESONANCE OBSERVATION

To understand the TREIT line shape one needs to consider the relative phase between the two optical fields, forming a two-photon EIT resonance [in our case, the carrier and the first modulation sidebands of the VCSEL laser, as shown in Fig. 1(a)]. While locally the two optical fields are nearly perfectly phase coherent, the value of their relative phase changes as the beams propagate, thanks to their frequency mismatch, at a rate given by Eq. (1). Thus, if the two beams travel unequal paths before entering the cell, the exact expressions for the atomic dark state in each beam will reflect the acquired phase difference, as illustrated in Fig. 1(b). For example, if we set the relative phase between two EIT fields as zero in the first beam and $\Delta\phi_{\mathrm{HF}}$ in the second beam, we can write the expressions for the unperturbed EIT dark states independently formed in each channel:

$$|D_1\rangle(t=0) = (\Omega_1|b\rangle - \Omega_0|c\rangle)/\Omega,$$
$$|D_2\rangle(t=0) = (\Omega_1|b\rangle - e^{i\phi_{\mathrm{HF}}}\Omega_0|c\rangle)/\Omega, \tag{2}$$

where Ω_0 and Ω_1 are the absolute values of Rabi frequencies for the two EIT transitions, and $\Omega = \sqrt{\Omega_0^2 + \Omega_1^2}$ is the normalization coefficient. In the case of zero two-photon detuning ($\delta = 0$) the optical response of the atoms, prepared in the dark state in one beam and then probed by another, is symmetric for both beams. However, a small two-photon detuning δ breaks this symmetry, since during the transit time τ between the two interactions the relative phases of the both dark states evolve by the same amount $\delta \cdot \tau$:

$$|D_1\rangle(t=\tau) = (\Omega_1|b\rangle - e^{i\delta\cdot\tau}\Omega_0|c\rangle)/\Omega,$$
$$|D_2\rangle(t=\tau) = (\Omega_1|b\rangle - e^{i\phi_{\mathrm{HF}}+i\delta\cdot\tau}\Omega_0|c\rangle)/\Omega, \tag{3}$$

causing the difference in optical responses depending on with which beam the atoms first interacted.

We can experimentally verify the significance of the EIT phase difference between the two beams by controlling the beam path for the second channel using a delay stage. Figure 3(a) shows the differential lock-in signal for the different delays. It is easy to see that it is possible to adjust the relative delay to almost perfectly match the EIT resonances in each channel (the small residual signal is due to small laser beam disbalance in two channels). However, by changing the delay

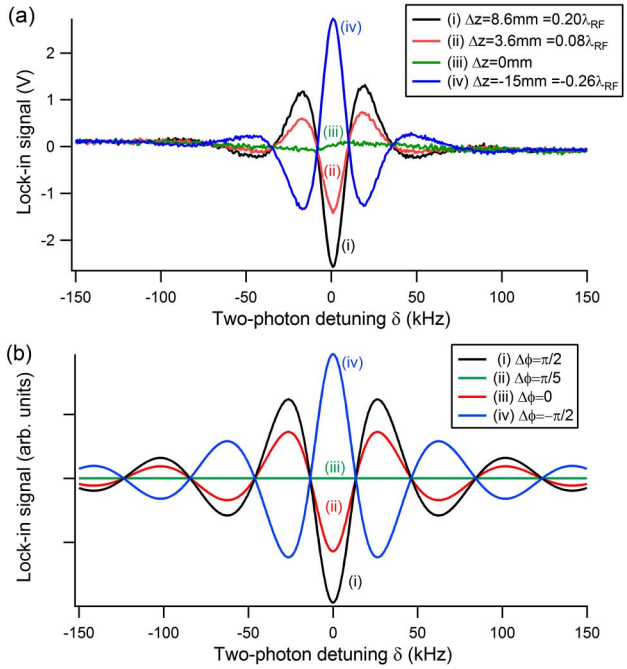

Fig. 3. (a) Differential lock-in signals as a function of the two-photon detuning for different relative prism position. Laser power in each channel is ≈50 μW. (b) Theoretical simulations of the lock-in readout of the differential TREIT signal using Eq. (4), assuming the beam diameter 0.8 mm, the distance between the beams 5 mm, optical Rabi frequency $\Omega_0 = 2\pi \cdot 8$ MHz and $\Omega_1 = 2\pi \cdot 3$ MHz.

one can maximize the contrast of the TREIT signal between the two channels.

We can qualitatively confirm such behavior using a repeated interaction model developed in [35,36] to describe the optical response of atoms after two consecutive interactions under EIT conditions. Generalizing this expression for the two regions with identical absolute values but different in phase EIT fields, we can describe the differential signal for a given travel time between the two beams τ as

$$\Delta I(\delta) \propto \frac{|\Omega|^2}{\delta^2+\Gamma^2} e^{-2\Gamma t_{\mathrm{tr}}} \sin\phi_{\mathrm{HF}} \times \sin[\delta(2t_{\mathrm{tr}}+\tau)+\tan^{-1}(\delta/\Gamma)], \quad (4)$$

where Γ is the power-broadened single-channel EIT linewidth and t_{tr} is the transit time of an atom through the interaction region. Here we neglect the intrinsic ground-state decoherence rate, which in our experiment is limited by the rate of the collisions with the cell's walls and is much smaller than $1/\tau$.

Figure 3(b) shows the results of numerical simulations for the differential lock-in signal, averaged over the transverse Maxwell–Boltzmann velocity distribution of atoms $v_\perp$. In this case each velocity group gives a weighted contribution into the overall optical response with its own transit time value $\tau(v_\perp) = d/v_\perp$, where d is the distance between the two beams. Despite many simplifications of the model (such as assuming optically thin medium, neglecting the Doppler broadening of optical transitions, and not taking into account the longitudinal motion of the atoms), the general features of the model predictions nicely match the experiment: we observe the maximum lock-in differential signal at zero two-photon detuning for $\phi_{\mathrm{HF}} = \pm\pi/2$, and the TREIT feature disappears for $\phi_{\mathrm{HF}} = 0$. Since in the calculations we assume only transverse motion of the atoms for simplicity, we somewhat underestimate the average transit time between the two beams, which leads to a small difference in the oscillation periods between the experimental and calculated signals.

4. SIGNAL-TO-NOISE ANALYSIS

Many EIT-based measurements suffer from the residual intensity noise, especially if broadband lasers, such as VCSELs, are used to excite optical transitions [37]. Several differential EIT schemes, e.g., based on magneto-optical rotation [38–41] or polarization selection rules [42], have been proposed recently to suppress the common-mode intensity noise while maintaining high-contrast EIT resonant features.

Our observations suggest that the TREIT signal may also be applied to reduce the intensity noise and thus boost the signal-to-noise ratio. Simple visual comparison of a single-channel EIT and TREIT signals in Fig. 1(d) shows a strong noise suppression in the differential signal. To quantify this observation, we measured the slope of each lock-in signal near zero two-photon detuning at the point where it crosses zero, as this slope determines the strength of the potential feedback error signal for the microwave frequency stabilization. A potential complication for the current detection method is that the lock-in zero-crossing frequency is shifted with respect to the exact atomic resonance. This may not be a problem for relative frequency measurements, but if such shift is not desired, it can be eliminated by employing the feedback scheme that oscillates between the two central zero-crossing locking points, thus effectively canceling the shift in the averaged frequency output. Alternatively, the second-harmonic error signal can be used.

The measured slope as a function of the laser power is plotted in Fig. 4(a). It is easy to see that both EIT schemes give comparable results. A single-channel EIT performs better at lower laser power, likely due to the reduced power broadening. Higher laser power, however, improves the optical pumping of atoms into the dark state, thus increasing the number of atoms contributing to the two-beam interactions. In addition, the Ramsey interrogation schemes are known to be less sensitive to the power broadening during the evolution in the dark period [22,23]. Thus, not surprisingly, the measured slope of the TREIT signal surpasses that of the single-channel EIT at higher laser powers.

At the same time, the comparison of the measured noise levels, shown in Fig. 4(b), clearly demonstrate the advantage of the differential detection, as we see more than an order of magnitude noise reduction for the differential TREIT signal.

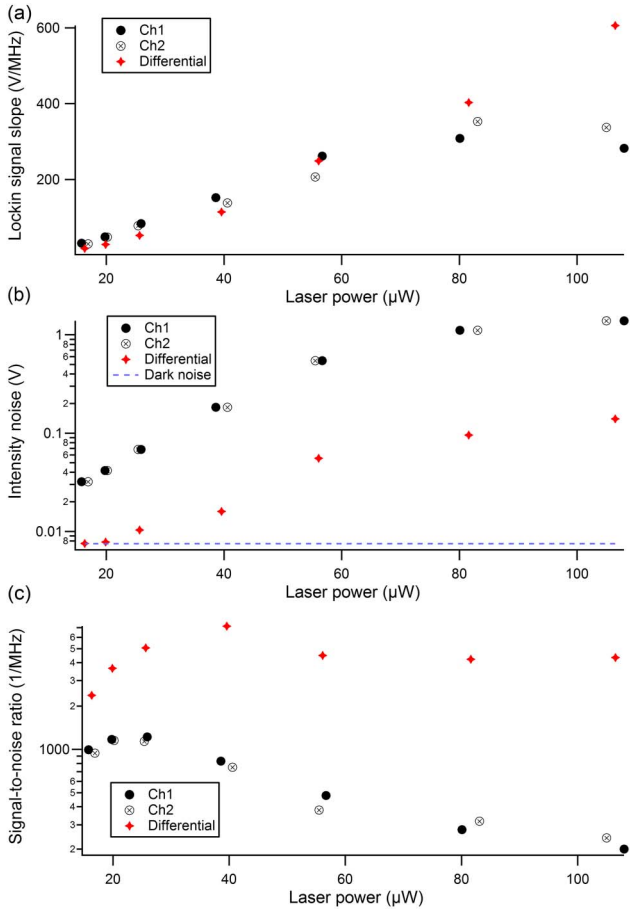

Fig. 4. Comparison of the one-channel EIT and TREIT performance. (a) Slope of the error lock-in signal for each optical channel and for the differential signal at the corresponding zero-crossing detunings. (b) Lock-in noise measured at zero-crossing two-photon position. Horizontal line shows the dark electronic noise level. (c) Signal-to-noise ratio (defined as slope of the error signal divided by the measure noise). For the differential measurements the average power between the two channel is used.

In fact, we were unable to accurately measure the TREIT noise for the lowest laser powers, as it fell below the technical noises of our detector. This is due to the cancellation of the common-mode intensity fluctuations under the TREIT detection, that dominate the noise in a single-beam detection.

The resulting SNR for both schemes is shown in Fig. 4(c). Note that while the SNR for the single-channel EIT has a clear maximum at approximately 30 μW of laser power due to the known saturation of the EIT amplitude at higher powers [33], the TREIT SNR remains relatively constant at high laser powers, which may be an attractive feature for some applications, especially if one employs more complex beam geometries to increase the number of atoms, participating in TREIT [27].

5. CONCLUSIONS

In this paper, we explored the possibility to effectively extend the spin coherence evolution time for thermal atoms inside a vapor cell by taking advantage of their ballistic motion between two spatially separated identical optical channels, undergoing consecutive Ramsey-like repeated interactions with the two beams. We demonstrated that such prolonged evolution of the spin coherence allows us to obtain a narrow differential signal on top of a regular EIT resonance, and showed that it is possible to either cancel or enhance the differential optical signal by controlling the relative phase between the two EIT fields in two regions, which sets the phase of the EIT dark states in each optical channel. Despite the relatively small percentage of atoms that fly through both beams before hitting the cell wall, their contribution in the overall optical transmission signal is not negligible and has to be taken into account for any experiments using the dual-rail arrangement. For example, we observed that when a phase-sensitive detection of the EIT resonances is employed, the signal due to the TREIT contribution is comparable to that of a regular EIT. At the same time, TREIT detection may offer significant advantages in signal-to-noise, as the intensity difference measurements suppresses the common intensity noise without sacrificing the strength of the feedback error signal.

Funding. National Science Foundation (NSF), Directorate for Mathematical and Physical Sciences (MPS) (PHY-308281).

Acknowledgment. We would like to thank Kelly Roman for the original exploratory work with two-beam EIT configuration, and Hana Warner and Kangning Yang for their help with the initial experiment construction. This research was supported by the National Science Foundation. R. M. J. acknowledges the support of the DeWilde research fellowship.

REFERENCES

1. M. D. Lukin, "Colloquium: trapping and manipulating photon states in atomic ensembles," Rev. Mod. Phys. **75**, 457–472 (2003).
2. K. Hammerer, A. S. Sørensen, and E. S. Polzik, "Quantum interface between light and atomic ensembles," Rev. Mod. Phys. **82**, 1041–1093 (2010).
3. A. I. Lvovsky, B. C. Sanders, and W. Tittel, "Optical quantum memory," Nat. Photonics **3**, 706–714 (2009).
4. K. Heshami, D. G. England, P. C. Humphreys, P. J. Bustard, V. M. Acosta, J. Nunn, and B. J. Sussman, "Quantum memories: emerging applications and recent advances," J. Modern Opt. **63**, 2005–2028 (2016).
5. L.-M. Duan, M. D. Lukin, J. I. Cirac, and P. Zoller, "Long-distance quantum communication with atomic ensembles and linear optics," Nature **414**, 413–418 (2001).
6. H. J. Kimble, "The quantum internet," Nature **453**, 1023–1030 (2008).
7. V. Boyer, A. M. Marino, R. C. Pooser, and P. D. Lett, "Entangled images from four-wave mixing," Science **321**, 544–547 (2008).
8. W. Wasilewski, T. Fernholz, K. Jensen, L. S. Madsen, H. Krauter, C. Muschik, and E. S. Polzik, "Generation of two-mode squeezed and entangled light in a single temporal and spatial mode," Opt. Express **17**, 14444–14457 (2009).
9. J. Vanier and C. Audoin, *The Quantum Phisics of Atomic Frequency Standards* (Adam Hilger, 1989), Vol. **1**.
10. J. Vanier, "Atomic clocks based on coherent population trapping: a review," Appl. Phys. B **81**, 421–442 (2005).
11. V. Shah and J. Kitching, "Chapter 2—advances in coherent population trapping for atomic clocks," in *Advances in Atomic, Molecular, and Optical Physics*, P. B. E. Arimondo and C. Lin, eds. (Academic, 2010), Vol. **59**, pp. 21–74.
12. D. Budker and D. F. J. Kimball, eds., *Optical Magnetometry* (Cambridge University, 2013).
13. M. Stahler, S. Knappe, C. Affolderbach, W. Kemp, and R. Wynands, "Picotesla magnetometry with coherent dark states," Europhys. Lett. **54**, 323–328 (2001).
14. D. Budker and M. Romalis, "Optical magnetometry," Nat. Phys. **3**, 227–234 (2007).
15. I. Novikova, R. L. Walsworth, and Y. Xiao, "Electromagnetically induced transparency-based slow and stored light in warm atoms," Laser Photonics Rev. **6**, 333–353 (2012).
16. D. Budker, V. Yashchuk, and M. Zolotorev, "Nonlinear magneto-optic effects with ultranarrow widths," Phys. Rev. Lett. **81**, 5788–5791 (1998).
17. M. Klein, M. Hohensee, D. F. Phillips, and R. L. Walsworth, "Electromagnetically induced transparency in paraffin-coated vapor cells," Phys. Rev. A **83**, 013826 (2011).
18. Y. Xiao, "Spectral line narrowing in electromagnetically induced transparency," Mod. Phys. Lett. B **23**, 661–680 (2009).
19. M. Fleischhauer, A. Imamoglu, and J. P. Marangos, "Electromagnetically induced transparency: optics in coherent media," Rev. Mod. Phys. **77**, 633–673 (2005).
20. E. Arimondo, "Coherent population trapping in laser spectroscopy," in *Progress in Optics*, E. Wolf, ed. (Elsevier, 1996), Vol. **35**, Chap. 5, pp. 259–354.
21. N. F. Ramsey, "A molecular beam resonance method with separated oscillating fields," Phys. Rev. **78**, 695–699 (1950).
22. T. Zanon, S. Guerandel, E. de Clercq, D. Holleville, N. Dimarcq, and A. Clairon, "High contrast ramsey fringes with coherent-population-trapping pulses in a double lambda atomic system," Phys. Rev. Lett. **94**, 193002 (2005).
23. N. Castagna, R. Boudot, S. Guerandel, E. Clercq, N. Dimarcq, and C. Clairon, "Investigations on continuous and pulsed interrogation for a cpt atomic clock," IEEE Trans. Ultrason. Ferroelectr. Freq. Control **56**, 246–253 (2009).
24. X. Liu, J.-M. Mérolla, S. Guérandel, E. de Clercq, and R. Boudot, "Ramsey spectroscopy of high-contrast cpt resonances with push-pull optical pumping in Cs vapor," Opt. Express **21**, 12451–12459 (2013).
25. Z. D. Grujić, M. Mijailović, D. Arsenović, A. Kovačević, M. Nikolić, and B. M. Jelenković, "Dark raman resonances due to Ramsey interference in vacuum vapor cells," Phys. Rev. A **78**, 063816 (2008).
26. H. Failache, L. Lenci, and A. Lezama, "Raman-Ramsey multizone spectroscopy in a pure rubidium vapor cell," Phys. Rev. A **81**, 023801 (2010).
27. I. S. Radojičić, M. Radonjić, M. M. Lekić, Z. D. Grujić, D. Lukić, and B. Jelenković, "Raman-Ramsey electromagnetically induced transparency in the configuration of counterpropagating pump and probe in vacuum Rb cell," J. Opt. Soc. Am. B **32**, 426–430 (2015).
28. A. Sargsyan, C. Leroy, Y. Pashayan-Leroy, R. Mirzoyan, A. Papoyan, and D. Sarkisyan, "High contrast *d* 1 line electromagnetically induced

transparency in nanometric-thin rubidium vapor cell," Appl. Phys. B **105**, 767–774 (2011).
29. A. Sargsyan, C. Leroy, Y. Pashayan-Leroy, S. Cartaleva, and D. Sarkisyan, "High-contrast dark resonances on the d1 line in cesium nanocell: the advantages compared with the other alkali *d* lines," J. Modern Opt. **62**, 769–777 (2015).
30. D. G. England, P. S. Michelberger, T. F. M. Champion, K. F. Reim, K. C. Lee, M. R. Sprague, X.-M. Jin, N. K. Langford, W. S. Kolthammer, J. Nunn, and I. A. Walmsley, "High-fidelity polarization storage in a gigahertz bandwidth quantum memory," J. Phys. B **45**, 124008 (2012).
31. D. B. Higginbottom, J. Geng, G. T. Campbell, M. Hosseini, M. T. Cao, B. M. Sparkes, J. Bernu, N. P. Robins, P. K. Lam, and B. C. Buchler, "Dual-rail optical gradient echo memory," Opt. Express **23**, 24937–24944 (2015).
32. M. Namazi, C. Kupchak, B. Jordaan, R. Shahrokhshahi, and E. Figueroa, "Ultralow-noise room-temperature quantum memory for polarization qubits," Phys. Rev. Appl. **8**, 034023 (2017).
33. E. E. Mikhailov, T. Horrom, N. Belcher, and I. Novikova, "Performance of a prototype atomic clock based on linlin coherent population trapping resonances in Rb atomic vapor," J. Opt. Soc. Am. B **27**, 417–422 (2010).
34. S. A. Zibrov, I. Novikova, D. F. Phillips, R. L. Walsworth, A. S. Zibrov, V. L. Velichansky, A. V. Taichenachev, and V. I. Yudin, "Coherent-population-trapping resonances with linearly polarized light for all-optical miniature atomic clocks," Phys. Rev. A **81**, 013833 (2010).
35. Y. Xiao, I. Novikova, D. F. Phillips, and R. L. Walsworth, "Diffusion-induced Ramsey narrowing," Phys. Rev. Lett. **96**, 043601 (2006).
36. Y. Xiao, I. Novikova, D. F. Phillips, and R. L. Walsworth, "Repeated interaction model for diffusion-induced Ramsey narrowing," Opt. Express **16**, 14128–14141 (2008).
37. J. C. Camparo and J. G. Coffer, "Conversion of laser phase noise to amplitude noise in a resonant atomic vapor: The role of laser linewidth," Phys. Rev. A **59**, 728–735 (1999).
38. B. Tan, Y. Tian, H. Lin, J. Chen, and S. Gu, "Noise suppression in coherent population-trapping atomic clock by differential magneto-optic rotation detection," Opt. Lett. **40**, 3703–3706 (2015).
39. X. L. Sun, J. W. Zhang, P. Cheng, C. Xu, L. Zhao, and L. J. Wang, "Investigation of Ramsey spectroscopy in a lin-par-lin Ramsey coherent population trapping clock with dispersion detection," Opt. Express **24**, 4532–4541 (2016).
40. M. A. Guidry, E. Kuchina, I. Novikova, and E. E. Mikhailov, "Characterization of frequency stability in electromagnetically induced transparency-based atomic clocks using a differential detection scheme," J. Opt. Soc. Am. B **34**, 2244–2249 (2017).
41. H. Lin, Y. Tian, B. Tan, and S. Gu, "Differential detection scheme for compact cpt atomic clocks," Europhys. Lett. **119**, 23001 (2017).
42. V. Gerginov, S. Knappe, V. Shah, L. Hollberg, and J. Kitching, "Laser noise cancellation in single-cell cpt clocks," IEEE Trans. Instrum. Meas. **57**, 1357–1361 (2008).